Published in final edited form as:
Ann Neurol. 2012 October ; 72(4): 525–535. doi:10.1002/ana.23652.

ISOFLURANE-INDUCED APOPTOSIS OF OLIGODENDROCYTES IN THE NEONATAL PRIMATE BRAIN

Ansgar M. Brambrink, MD, PhD[1,2,7], **Stephen A. Back, MD, PhD**[1,2,3,7], **Art Riddle, Ph.D.**[3], **Xi Gong, M.D.**[3], **Matthew D. Moravec, B.A.**[3], **Gregory A. Dissen, PhD**[4], **Catherine E. Creeley, PhD**[5], **Krikor T. Dikranian, MD, PhD**[6], and **John W. Olney, MD**[5]

[1]Department of Anesthesiology and Perioperative Medicine, Oregon Health and Science University, Portland, OR

[2]Department of Neurology, Oregon Health and Science University, Portland, OR

[3]Department of Pediatrics, Oregon Health and Science University, Portland, OR

[4]Oregon National Primate Research Center, Division of Neuroscience, Beaverton, OR

[5]Department of Psychiatry, Washington University School of Medicine, St. Louis, MO

[6]Department of Anatomy and Neurobiology, Washington University School of Medicine, St. Louis, MO

Abstract

Objective—Previously we reported that exposure of 6-day old (P6) rhesus macaques to isoflurane for 5 hours triggers a robust neuroapoptosis response in developing brain. We have also observed (unpublished) that isoflurane causes apoptosis of cellular profiles in the white matter that resemble glia. We analyzed the cellular identity of the apoptotic white matter profiles and determined the magnitude of this cell death response to isoflurane.

Method—Neonatal (P6) rhesus macaques were exposed for 5 hours to isoflurane anesthesia according to current clinical standards in pediatric anesthesia. Brains were collected 3 hours later and examined immunohistochemically to analyze apoptotic neuronal and glial death.

Results—Brains exposed to isoflurane displayed significant apoptosis in both the white and gray matter throughout the CNS. Approximately 52% of the dying cells were glia, and 48% were neurons. Oligodendrocytes (OL) engaged in myelinogenesis were selectively vulnerable, in contrast to OL progenitors, astrocytes, microglia and interstitial neurons. When adjusted for

Correspondence to: Stephen A. Back, M.D., Ph.D., Oregon Health and Science University, Biomedical Research Building, L481, 3181 S.W. Sam Jackson Park Rd., Portland, Oregon 97239-3098, Phone: 503-494-0906, backs@ohsu.edu. Ansgar Brambrink, M.D., Ph.D., Oregon Health & Science University, 3181 SW Sam Jackson Park Road, Portland, OR 97239-3098, Phone: (503) 494-5210, Fax: (503) 494-3081, brambrin@ohsu.edu.
[7]These joint-senior authors contributed equally to this work

Author Contributions: A.M.B. was responsible for all animal studies, quantitation of cell proliferation and quantitative analysis to optimize cell degeneration detection by AC3 vs. Hoechst. G.A.D. directed the veterinary care of the animals. C.C. supervised tissue processing and all histological studies for light microscopy by AC3 and silver staining that first identified glioapoptosis in the lab of JWO. K.T.D. performed immunohistochemical studies to rule out apoptosis of astrocytes and to document lack of an astrogliosis response to isoflurane. In the lab of S.A.B., X.G. and M.D.M. were responsible for fluorescence immunohistochemical studies to define the susceptibility of the OL lineage and other glia and A.R. performed confocal microscopy studies that defined the OL lineage stages susceptible to injury, axonal susceptibility to injury and cell proliferative responses within the OL lineage. S.A.B. proposed, designed and evaluated the immunohistochemical and quantitative studies that defined the susceptibility of OLs to apoptosis relative to other cell types in white matter. J.W.O as principal investigator conceived the project and together with A.M.B. and S.A.B., as co-principal investigators, were responsible in their respective labs for conducting and directing the work, data analysis and interpretation, and manuscript preparation. All authors contributed to the writing of the manuscript.

control rates of OL apoptosis, the percentage of OLs that degenerated in the forebrain white matter of the isoflurane-treated group was 6.3% of the total population of myelinating OLs.

Interpretation—Exposure of the infant rhesus macaque brain to isoflurane for 5 hours is sufficient to cause widespread apoptosis of neurons and OLs throughout the developing brain. Deletion of OLs at a stage when they are just beginning to myelinate axons could potentially have adverse long term neurobehavioral consequences, that might be additive to the potential consequences of isoflurane-induced neuroapoptosis.

Acute exposure to specific classes of drugs, including those that block NMDA glutamate receptors, those that activate $GABA_A$ receptors, and ethanol (which has both NMDA antagonist and GABA-mimetic properties), triggers widespread apoptotic death of neurons in the developing brain of several species, including rats,[1–4] mice,[5] guinea pigs[6], piglets[7], and non-human primates.[8–13] The window of peak vulnerability to the apoptogenic mechanism coincides with the developmental period of rapid synaptogenesis,[1,2] also known as the brain growth spurt period, which occurs primarily during the first 2 weeks after birth in mice and rats, but in humans extends from about mid-gestation to several years after birth.[14]

The above findings have potential human relevance, because it is not uncommon for the developing human brain to be exposed to drugs that have NMDA antagonist or GABA-mimetic properties. The list includes numerous agents that are sometimes abused by pregnant mothers (ethanol, phencyclidine, ketamine, nitrous oxide, barbiturates, benzodiazepines) and many that are used worldwide in obstetric and pediatric medicine (anticonvulsants, sedatives and anesthetics). Anesthetic drugs are currently the focus of intense interest, because of mounting evidence that even single or brief exposure to clinically relevant doses of commonly used anesthetics (ketamine, midazolam, propofol, isoflurane, sevoflurane, chloral hydrate) may trigger a significant neuroapoptosis response in the developing rodent brain,[15–20] and exposure of the developing rodent brain to these agents can result in long-term neurobehavioral impairments.[4,21–28] Moreover, there is emerging evidence potentially linking anesthesia exposure in infancy with long-term neurobehavioral deficits in both human[29–35] and non-human[36] primates.

Research aimed at clarifying whether anesthetic drugs can trigger neuroapoptosis in the neonatal non-human primate (NHP) brain includes studies by Slikker and colleagues[8–10] who reported that exposure of the postnatal day 5 (P5) rhesus macaque brain to ketamine for 24 or 9 hours, or to a combination of nitrous oxide and isoflurane for 8 hours, triggered a significant neuroapoptosis response. We have shown that exposure of the P6 neonatal rhesus macaque brain to either ketamine[12] or isoflurane[11] for 5 hours triggered apoptotic neurodegeneration, but there are no reports describing apoptosis of glial cells following exposure to any anesthesia protocol. In P6 rhesus neonates exposed to isoflurane we have observed (unpublished) an apoptosis response in white matter cells that morphologically resemble glia. The present study was undertaken to clarify the identity of the white matter cells that undergo apoptosis following isoflurane exposure and to determine the magnitude of this cell death response.

Methods

Animals and Experimental Procedures

All animal procedures were approved by the Oregon National Primate Research Center and Washington University Medical School Institutional Animal Care and Use Committees and were conducted in full accordance with the PHS Policy on Humane Care and Use of Laboratory Animals. Isoflurane anesthesia was administered to the infant monkeys with the

same standard of care that is practiced in a state-of-the-art pediatric operating room. An abbreviated description of these methods is given below and a more detailed description is presented in the Supplementary Materials section. Supplemental Table 1 demonstrates that the physiological responses to isoflurane were within the normal range and equivalent to those observed in pediatric anesthesiology practice.

Six day-old (P6) infant rhesus macaques (n=5/group) were exposed for 5 hours either to room air or to isoflurane maintained at a concentration that provided a moderate plane of surgical anesthesia as defined by no movement and not more than 10% increase in heart rate or blood pressure in response to a mosquito clamp pinch at hand and foot (checked every 30 min). Based on the work of Dobbing and Sands,[14] we estimate that the P6 rhesus infant is the neurodevelopmental equivalent of a 4–6 month old human infant. After 5 hours of isoflurane anesthesia and a 3-hour observation period in an animal incubator, the animals received high-dose phenobarbital and were transcardially perfusion-fixed to prepare the brain for histopathological analysis. No complications occurred during in-vivo tissue fixation.

Histopathology Studies

After in vivo perfusion fixation with 4% paraformaldehyde in phosphate buffer, 70 μM serial coronal sections were cut on a vibratome across the entire rostro-caudal extent of the forebrain, midbrain, brain stem and cerebellum. Sections were selected at 2 mm intervals (~30 sections/brain) and stained by the DeOlmos cupric silver method (marks dying cells) or by activated caspase 3 (AC3) immunohistochemistry, as described previously.[5,8–13,15–22,37] The non-fluorescent AC3 staining method permits comprehensive quantification of apoptotic profiles in isoflurane-exposed vs. control brains. It provides a permanent record of the cell death pattern throughout the brain, and also robustly stains both cell bodies and processes, which allows one to distinguish early from late stages of degeneration. Moreover, the diaminobenzidine (DAB) amplification provides a sensitive means to detect AC3-positive cells. In previous studies, we focused attention exclusively on gray matter and included in our quantitative counts only those AC3-positive profiles with neuronal morphology. However, we have consistently observed abundant AC3-positive profiles in white matter tracts of isoflurane-exposed brains that have a distinctive morphological appearance resembling glia. We applied a battery of cell-type specific markers to identify what glial cell types co-labeled for AC3.

Analysis of Glial Cell Death—To clarify whether the degenerating glial profiles might be astrocytes or microglia, we double-stained for AC3 and GFAP (marker for astrocytes) or Iba1 (marker for microglia and macrophages). Because the morphology of many of the AC3-labeled cells in the white matter resembled cells derived from the oligodendrocyte (OL) lineage, we visualized multiple markers that identify successive OL lineage stages. The stages distinguished were the OL progenitor, the preOL (late OL progenitor) the immature OL and the mature OL. Myelination is initiated by the immature OL and proceeds through the mature OL stage. Markers employed for detecting OL lineage cells have the following properties. The platelet-derived growth factor receptor alpha (PDGFRα) localizes to the

plasma membrane of OL progenitors. The O1 and O4 monoclonal antibodies stain the plasma membrane of preOLs (O4+O1−) and immature OLs (O4+O1+) as well as myelin sheaths (O4+O1+). Olig 2 is a nuclear transcription factor expressed by all OL stages. CC-1 is a cytoplasmic marker that stains the cytoplasm of mature OLs but has been detected in post-mitotic cells that stain with markers for earlier stages of the OL lineage.[38]

Immunofluorescent detection of caspase-mediated cell death employed an activated caspase-3 (AC3) rabbit polyclonal antisera (9661B; 1:500; Cell Signaling Technology, Inc., Danvers, MA) that was incubated overnight with tissue sections at 2–4°C. The AC3 antisera was next incubated for 2 hr at room temperature (RT) with biotinylated goat anti-rabbit IgG (1:200; 111-065-0465; Jackson ImmunoResearch West Grove, PA) and visualized with rhodamine red X-conjugated streptavidin (1:400, RT; 016-290-084, Jackson ImmunoResearch). Since the O4 and O1 staining is disrupted by detergents and antigen retrieval, these treatments were not employed. The O4 and O1 antibodies were co-incubated with the AC3 antibody as described above. Detection of the O4 and O1 antibodies was done as previously described for human fetal tissue.[39] Double-staining for AC3 and PDGFRα employed a goat antisera against PDGFRα (1:6; 0.3% TritonX-100; antigen retrieval at pH 9.0, as described below; five-night incubation at 2–4°C; AF-307-NA; R & D systems; Minneapolis, MN). Double-staining for AC3 and Olig 2 employed a mouse monoclonal antibody against Olig 2 (1:10,000; 0.1% Triton; a generous gift from Dr. John Alberta, Dana Farber Cancer Institute, Boston, MA). Double staining for AC3 and CC-1 employed a mouse monoclonal antibody against CC-1 (1:200; 0.1% Triton; OP80; Calbiochem, San Diego, CA). Tissue was pre-treated with antigen retrieval (10 mM Trizma-Base, 1 mM EDTA, pH 9.0; 90°C, 10 min) for detection of Olig 2 and CC-1. Double-staining for AC3 and GFAP employed a mouse monoclonal antibody against GFAP (1:500; Mab360; Millipore, Temecula, CA). Microglia were visualized with a rabbit polyclonal antiserum against Iba1 (019-18741; 1:500 in PBS with 0.1% triton X-100; Wako Chemicals, Richmond, VA).

Cell proliferation was determined by immunohistochemical detection of the mouse monoclonal antibody Ki67 (1:200; NCL-L-Ki67-MM1; Leica Biosystems Newcastle Ltd, United Kingdom), which required antigen retrieval (10 min in 50mM sodium citrate, pH 6.0 at 90°C). Axon degeneration was analyzed with the anti-neurofilament antibody, SMI-312 (1:1000; Covance, Emeryville, CA) and with the rabbit polyclonal antisera (Fractin) that detects caspase-cleaved actin (KYEAb4; 1:400, generous gift of Dr. Greg Coles, VA Medical Center, UCLA). To visualize integrity of the nodes of Ranvier, we detected the paranodal contactin-associated protein (Caspr), a component of axo-glial junctions. After antigen retrieval, sections were incubated with a mouse monoclonal antibody against Caspr (1:500; 75-001; NeuroMab, Davis, CA) for 3 days at 4 °C in PBS with 0.1% Triton X-100, 3% NGS. Tissue sections were counterstained with Hoechst 33342 to visualize nuclear morphology and define regional boundaries.

Quantification of apoptosis and regenerative response

AC3-positive neuronal profiles, visualized by immunoperoxidase staining were counted by an investigator who was blinded to the treatment condition. Each entire stained section was analyzed by light microscopy using a 10× objective lens and a computer-assisted Stereo Investigator system (Microbrightfield Inc., Williston, VT) with an electronically driven motorized stage. In each section the identity and location of each AC3 stained profile was plotted. The rater used color-coding and, on the basis of location and morphological appearance, plotted each stained profile as either a red dot (neuron) or green dot (glia). The total area scanned and the total number of stained neurons or glia per section and per brain were computer-recorded. White matter boundaries were also defined to calculate the density of AC3 profiles in the white matter. From the recorded information, the density of apoptotic profiles per mm^3 was estimated for the entire brain or for any given region within the brain, and the total number of apoptotic profiles in the entire brain was also estimated. In addition, a computer plot showing the regional distribution of stained profiles was generated and the plots for each region of each brain for each treatment condition were compared.

To quantify the percentage of cells that degenerated in the frontal corona radiata in controls (n=5) and isoflurane-exposed (n=5) animals, a minimum of three adjacent sections were immuno-fluorescently stained for AC3 and CC1 and counterstained with Hoechst 33342, as described above. These sections were also analyzed to compare the sensitivity of AC3 and Hoechst to detect degenerating cells. The Hoechst counterstain was also used to define gray-white matter boundaries within the corona radiata and to ensure that cell counts were uniformly sampled throughout the white matter. Cells were counted on an upright fluorescent microscope with a 40× objective equipped with a counting grid (0.0625 mm^2/field). AC3-labeled cells that contained a nucleus with features of typical apoptotic degeneration (condensed or fragmented nucleus) were defined as degenerating cells. A minimum of 10 fields were counted in each tissue section. Cells with atypical appearing nuclei (e.g., fusiform or sickle shaped nuclei) were also counted and categorized separately. No significant differences in the density of these atypical nuclei were found for the control and experimental groups and these counts were not included in the analysis. The total number of mature OLs at risk for degeneration in both groups was determined from counts of CC1-labeled cells. The percentage of degenerating cells was calculated from the ratio of the density of AC3- or Hoechst-labeled cells (numerator) and the density of CC1-labeled cells (denominator).

To quantify the density of cells that proliferated in response to isoflurane exposure, tissue sections were immunofluorescently doubled-stained for Ki67 and AC3 and counterstained with Hoechst, as described above. Cell counts were done with a 40× objective (see above). Counts were done in a minimum of 10 randomly selected fields within two regions of interest—those containing at least one AC3-labeled cell and those that lacked AC-3 staining. This strategy was designed to determine whether cell proliferation was preferentially associated with regions of cell degeneration.

Statistical Analysis

Data are presented as mean ± standard error of the mean (SEM). Student's t-test with Welch correction, where appropriate, was used. A two-sided P value less than 0.05 was judged significant and the 95% confidence interval for the mean difference provided a measure of precision. Statistical analysis was performed with Prism, GraphPad Software, Inc.

Results

Response to isoflurane exposure

The experimental protocol was well tolerated by all NHP infants. Each animal randomized to isoflurane exposure survived induction and maintenance of anesthesia. The concentration of the volatile anesthetic was maintained at the desired levels (endtidal 0.7–1.5 Vol%; n=5). Vital signs, blood gases and metabolic values remained within normal limits throughout the entire experimental period (Supplemental Table 1). The infant macaques quickly recovered after cessation of isoflurane delivery and were extubated to room air within 10 minutes without complications. All infants tolerated formula milk within two hours after cessation of isoflurane.

Isoflurane-induced glial degeneration in neonatal cerebral white matter

Qualitative histopathological evaluation of brains stained for AC3 (Fig. 1A–C) or by the DeOlmos cupric silver stain (Fig. 1D) each revealed cell death in cerebral white matter tracts. These degenerating cells appeared to be much more abundant in the isoflurane-exposed white matter, and had morphological features consistent with glia. Some of the AC3-stained profiles appeared to be in an early stage of degeneration (Fig. 1B, C) and others appeared to be in a more advanced stage (Fig. 1A; arrows). All of the silver-stained profiles

(Fig. 1D) appeared to be in a late stage, consistent with the fact that the degeneration products detected by silver typically localize to cells at advanced stages.

By immunofluorescent double-labeling, the AC3-staining in the white matter did not co-localize to cells with morphological features of degeneration as defined by NeuN (neuronal marker; Fig. 2A) or GFAP (astrocyte marker; Fig. 2B). Iba1-labeled microglia-macrophages (Fig. 2C, D) typically appeared activated within regions of cell degeneration and contained degenerating nuclear fragments, consistent with phagocytosis. OL progenitors visualized with the marker PDGFRα did not co-localize with AC3 (Fig. 2E) or with apoptotic-appearing nuclei visualized with Hoechst 33342 (Fig. 2F; arrows).

Acute White Matter Responses to Isoflurane Exposure

We next determined whether early reactive or regenerative responses occurred in the white matter during the short 8-hour survival time after the beginning of the isoflurane exposure. There was no apparent astroglial activation in the isoflurane-treated animals compared to controls (Supplemental Fig. 1).

We employed three approaches to determine if isoflurane exposure triggered early axonal degeneration. There was no apparent axonal degeneration visualized by staining for the axonal neurofilament protein marker SMI-312 (Supplemental Fig. 2A,B), a sensitive indicator of axonal injury in developing white matter.[40] The architecture of the nodes of Ranvier also did not appear to be disrupted. Myelinating neonatal white matter is enriched in nodal and paranodal proteins.[41] We visualized the distribution of the paranodal contactin-associated protein (Caspr), a component of axo-glial junctions, which is situated adjacent to the nodes of Ranvier. Supplemental Figure 2C demonstrates that isoflurane treatment did not disrupt the distribution of Caspr. We also visualized caspase-cleaved actin, which is a marker of axonal degeneration and apoptotic cells in necrotic foci of perinatal white matter injury.[42,43] The fractin antibody visualized degenerating apparent apoptotic OLs in the white matter, but no fractin-labeled axons were detected (Supplemental Fig. 2D).

To determine if isoflurane triggered cell proliferation, we visualized the distribution of the proliferation marker Ki67 in the frontal corona radiata. We observed a modest but significant increase in the density of Ki67-labeled nuclei in isoflurane-treated animals (62 ± 5 nuclei/mm^2; mean ± SEM) vs. control (30 ± 4; $p<0.001$). These nuclei were randomly distributed throughout the white matter and were not enriched in association with AC3-labeled cells. The proliferative cell population did not appear to originate from microglia, as assessed by double-staining for Ki67 and Iba1. Double-staining for Ki67 and the pan-oligodendrocyte marker Olig2 visualized a small proliferative subpopulation of oligodendrocyte lineage cells in both the control and isoflurane treated animals (Supplemental Figure 3). Approximately half of the Ki67-labeled nuclei co-localized with Olig2 in both control and isoflurane-treated animals. Hence, isoflurane exposure did not trigger early reactive astrogliosis or axonal degeneration, but was associated with a modest diffuse proliferative response.

Degenerating glia are pre-myelinating and myelinating oligodendrocytes (OLs)

We found extensive early myelination present within the neonatal NHP cerebral white matter tracts, as visualized with the O4 and O1 antibodies, which bind to lipid constituents in the plasma membrane of OL lineage cells and the surrounding myelin sheaths (Fig. 3A). At the periphery of the myelinating tracts, individual immature OL somata and processes were often visualized (Fig. 3B). Within white matter tracts, OL somata were also visualized by epi-fluorescence microscopy, but were more difficult to distinguish from the dense myelin surround (Fig. 3C). However, by confocal microscopy, AC3-positive profiles were

visualized with morphological features of OLs (Fig. 3D), as confirmed by a rim of O4 staining that localized to the plasma membrane (Fig. 3E) and coincided with AC3 (Fig. 3F).

To determine whether degenerating mature OL somata were present in the myelinated tracts, we next double-labeled for AC3 and CC-1, a mature OL marker with a cytoplasmic distribution. CC-1 was strongly expressed in numerous non-degenerating cells both within the control (not shown) and isoflurane-treated white matter (Fig. 4A). By epi-fluorescence microscopy CC-1 did not appear to localize to the AC3-labeled cells that resembled OLs (Fig. 4A). Similarly, Olig 2 (a pan-OL lineage marker) also was strongly expressed in numerous non-degenerating nuclei, but did not appear to co-localize with AC3-positive profiles by epi-fluorescence microscopy (Fig. 4C). However, confocal microscopy revealed that expression of both CC-1 (Fig. 4B) and Olig2 (Fig. 4D) was detectable to a variable degree within degenerating AC3 labeled cells, and the level of expression appeared to be dependent on whether the OL was in an early or late stage of degeneration. In those cells that retained morphological features indicative of an early stage, staining for CC-1 or Olig2 was detectable, but was not detected in those cells that appeared to be in a late stage of degeneration. Thus, the CC-1 and Olig2 antigens appeared to be subject to loss of immunoreactivity relatively early in the course of apoptosis.

Quantitative assessment of caspase-mediated neuronal and OL degeneration

Quantitative evaluation of AC3-stained sections from the brains exposed to isoflurane (n = 5) revealed that the mean (± SEM) number of all AC3-positive profiles (neurons + glia) per brain was $40.03 \times 10^5 \pm 6.69 \times 10^5$, and in the five control brains was $3.17 \times 10^5 \pm 0.85 \times 10^5$ (Fig. 5). Hence, there was a 12.6-fold increase in the number of apoptotic profiles in the isoflurane-exposed brains compared to the brains from drug-naive controls. The difference in the mean number of apoptotic profiles between the isoflurane and control groups was 36.86×10^5 (95% confidence interval, 55.4×10^5 to 18.3×10^5, p=0.005). In the isoflurane-treated group, the mean number of AC3-positive neuronal profiles was 19.14×10^5 and the mean number of AC3-positive glial profiles was 20.89×10^5, which yields a ratio of degenerating neurons to glia of 48:52.

We also made a quantitative comparison between the density of AC3-positive OLs in the isoflurane-exposed brains and the density of non-degenerating OLs in control brains, as detected by CC-1 staining. This estimate is based on an analysis that sampled throughout the frontal corona radiata, an extensive region of cerebral white matter that had a relatively prominent OL death response that is representative of most cerebral white matter regions (see Figs. 6 and 7). The mean density of AC3-positive glial profiles in the isoflurane-exposed group was 57 ± 3 cells/mm^2 and was significantly increased relative to controls (5 ± 1; p<0.0001).

We next considered the possibility that AC3 staining may fail to detect some of the OLs that degenerate following isoflurane exposure, especially those that have lost immunoreactivity because they are in a late stage of cell death. Therefore, as an alternate means of estimating the magnitude of OL apoptosis, we counted Hoechst-positive nuclear profiles showing typical apoptosis changes (condensation and fragmentation of nuclear chromatin) in the same regions of white matter where AC3 was quantified. The mean density of Hoechst-positive apoptotic nuclei in the isoflurane-exposed group was 96 ± 7 cells/mm^2, and was significantly increased relative to controls (9 ± 1; p<0.0001).

Because Hoechst staining detected a larger number of degenerating OLs in both the isoflurane and control brains, we decided to use the Hoechst values for estimating the magnitude of the OL response to isoflurane. To define the total OL population at risk of degeneration, we determined that the mean density of CC-1-positive OLs was 1357 ± 30

cells/mm^2 in the isoflurane-treated group, which did not differ significantly from controls (1143 ± 23 cells/mm^2). These data indicate that of the total OL population at risk, 7.1% (96 as a percentage of 1357) underwent apoptosis in the isoflurane-exposed brains versus 0.8% (9/1143) in the control brains. Subtracting the control value, which represents cells dying by natural apoptosis, yields 6.3% as the magnitude of the apoptosis response that can be attributed to isoflurane exposure.

Isoflurane induces diffuse neuronal and OL degeneration

The distribution and histological appearance of AC3 stained neurons in isoflurane-exposed brains was illustrated in a prior publication.[11] Figure 6 provides computer plots that demonstrate the relative typical diffuse distribution of AC3-positive neurons (red) and glia (green) at two representative levels in the cerebral cortex (a mid rostro-caudal level in A, B and the level of the primary visual cortex in C, D). The AC3-positive glia were highly enriched in the white matter. Figure 7 demonstrates in AC3-stained sections that at all levels of the neuraxis there were degenerating glial profiles with the same histological appearance as those shown in the corpus callosum in Figure 1. The glial degeneration in the internal capsule and frontal corona radiata was representative of that observed at the levels of the prefrontal, parietal, temporal and occipital cortices. Glial degeneration was not restricted to the cerebral hemispheres, but was also observed in the diencephalon (e.g., the optic tract), the midbrain (e.g., the cerebral peduncle) and hindbrain (e.g., cerebellar peduncle and medial lemniscus).

Discussion

Our findings document that a moderate surgical plane of anesthesia maintained by isoflurane for 5 hours is sufficient to cause a robust apoptotic cell death response affecting both neurons and glia in the neonatal NHP brain. Isoflurane-induced neuroapoptosis has been described previously,[11] but this is the first report describing isoflurane-induced glio-apoptosis. The glial cell type that was selectively affected were oligodendrocytes, which are highly enriched in actively myelinating neonatal white matter but are uncommon at this age in cerebral gray matter. OL progenitor stages were not affected, nor were other glial cell types, interstitial neurons or axons.

We estimated that the number of OLs deleted from the neonatal NHP brain by a single exposure to isoflurane may be in the range of 6.3% of the total population of myelinating OLs. This estimate was derived from analysis of a large region of frontal cerebral white matter in the corona radiata, a region that is representative of many other cerebral white matter zones. Although our findings document that OL degeneration occurs diffusely throughout brain white matter tracts, additional studies are needed to define differences that may be region-specific and developmental age-dependent. Our estimate of isoflurane-mediated OL degeneration was limited by the currently available methods to quantify cell death and the survival time of the animals after isoflurane exposure. First, we relied on Hoechst staining to quantify OL degeneration. Hoechst detected more OL degeneration than did AC3, but OLs in early stages of apoptosis may be detected by AC3 but not Hoechst. Given that AC3 and Hoechst have partially overlapping sensitivity to detect different stages in the cell death continuum, either marker may underestimate total OL loss. Secondly, our analysis was limited to a single early survival time at 3 hours after cessation of isoflurane exposure, designed to capture an early wave of apoptosis. However, OL apoptosis may persist during later intervals. Thirdly, the denominator used to calculate the percentage of OL death may be too large, in that it relied on CC-1 staining, which in adult mice, labels both myelinating OLs and at least some OL progenitors.[38] However, our preliminary studies using double-staining for CC-1 and PDGFRα found no CC-1 expression in OL progenitors

from neonatal NHP. Hence, our estimate of OL degeneration may possibly underestimate the total burden of cell death.

The biological consequences of deleting myelinating OLs from the developing brain remain to be determined, but may include disruption of myelinogenesis and pathological changes in axonal structure or function. Given that a single OL myelinates multiple axons, OL apoptosis may focally disrupt myelination and nerve conduction for multiple axons within the field of a single OL. If pathological changes occur, it is not known whether they are permanent or transitory, and whether recovery mechanisms can reverse such changes. We did not detect structural axonal pathology or reactive astrogliosis, but 3 hours after cessation of isoflurane exposure may be too early to detect such changes. We observed a mild proliferative response from OL lineage cells and other cell types, and early phagocytosis of degenerating OLs by microglia. The activation of microglia may promote neuro-inflammation, which may further compromise OL maturation and myelination in neonatal white matter.[44]

It is noteworthy that OL degeneration induced by isoflurane differs from OL degeneration associated with perinatal hypoxia/ischemia, in that the latter primarily entails initial loss of pre-myelinating OL progenitors,[42,45] by a mechanism that is primarily excitotoxic (necrotic), as opposed to caspase 3-mediated apoptosis. It is not known how long the window of vulnerability remains open for anesthesia-induced apoptosis of neurons or OLs, but developmental age at time of isoflurane exposure could possibly influence the potential for recovery. An important challenge for future research is to define the window of vulnerability to anesthesia-induced apoptosis for both neurons and OLs, and to develop a better understanding of the recovery potential inherent in each type of injury.

It has long been assumed that anesthetic drugs are safe for the developing brain, but new questions have been raised by recent human studies[29–32] documenting a significant association between a single brief exposure to anesthesia in infancy, and subsequent neurobehavioral disturbances. Other recent human studies found that a single exposure was not sufficient, but two or more brief anesthesia exposures prior to two years of age was associated with a significantly increased risk for learning disabilities,[33,34] and attention deficit/hyperactivity disorder.[35] Regardless whether a single exposure is sufficient, multiple exposures might entail cumulative OL loss and, perhaps, progressive axonal pathology which, together with cumulative loss of neurons, could potentially play a role in subsequent neurobehavioral disturbances.

While the majority of full term human infants who require anesthesia are not exposed multiple times, this is not true for premature or full-term infants in neonatal intensive care units (NICU) worldwide who are often exposed to light anesthesia (procedural sedation) intermittently or sometimes continuously for a period of days or weeks. These infants may also receive deep anesthesia for surgery, and some may be exposed to anti-epileptic drugs (AEDs) on a repetitive basis. Valproate is one of the more potent AEDs that triggers neuroapoptosis in developing rodent brain.[3] Recent human studies found that daily exposure of human fetuses to valproate during the third trimester of pregnancy is associated with a 9 to 12 point deficit in IQ.[46,47] Premature human infants are at the same neurodevelopmental age as third trimester fetuses. It is well recognized that premature human infants have a high incidence of behavioral delays and neurocognitive difficulties in grade school,[48] but anesthesia exposure in the NICU has received no attention as a potential contributory factor. Although our findings are particularly relevant to more mature and myelinated white matter, OLs and myelination are detected in fetal cerebral white matter during the second trimester.[39,49] Our preliminary data support that the window for isoflurane toxicity extends to OLs in preterm NHP white matter.

A major objective of NHP studies pertaining to the toxic effects of anesthetic drugs on the developing brain is to determine whether there are some anesthesia protocols that pose more risk than others. We recently reported that a 5-hour exposure of the neonatal NHP to ketamine (NMDA antagonist) causes a neuroapoptosis response that was only 1/3 as great as that observed here for isoflurane.[12] This suggests that when ketamine or isoflurane are administered to NHP infants in a manner that provides approximately the same depth and duration of anesthesia, isoflurane may have a greater adverse impact on the developing brain than ketamine. However, future studies will be required to evaluate the relative effects of these agents on long-term neurocognitive outcomes.

A potential explanation for the severity of isoflurane's apoptogenic action would be that it has both $GABA_A$ agonist and NMDA antagonist properties.[50,51] This interpretation is consistent with evidence from rodent studies that anesthesia protocols comprising a combination of these two classes of drugs, cause more severe neuroapoptosis and/or neurobehavioral disturbances.[4,17,25] Alcohol, which has both NMDA antagonist and $GABA_A$ agonist properties, causes a particularly severe neuroapoptosis reaction in both the infant rodent[2,5] and fetal NHP brain,[13] and alcohol is well known to have deleterious effects on the fetal human brain [fetal alcohol spectrum disorder (FASD)].[52] Also noteworthy is evidence that alcohol, like isoflurane, causes both neuroapoptosis[13] and oligoapoptosis[53] (manuscript in preparation), and that both alcohol[13] and isoflurane cause severe damage in the NHP basal ganglia, which coincides with evidence that loss of neuronal mass in the basal ganglia is a consistent finding in patients diagnosed with FASD.[52,54] Similarly, recent neuroimaging evidence documents loss of neuronal mass in the basal ganglia of human patients exposed during the third trimester of pregnancy[55] to anti-epileptic drugs (AEDs) that have apoptogenic properties resembling those of alcohol and isoflurane[3]. The potential of AEDs and sedative/anesthetic drugs to induce neuronal or glial apoptosis in specific regions of the developing brain may adversely influence the development of infants with a variety of neurogenetic or acquired disorders that also compromise these same brain regions.

In summary, exposure of the infant rhesus macaque brain to isoflurane anesthesia for 5 hours was associated with a relatively low magnitude but widely dispersed increase in apoptotic death of neurons and OLs engaged in myelinogenesis. These findings have potential human relevance in that recent clinical studies[29–35] suggest that brief anesthesia exposure of human infants, especially if it occurs two or more times prior to two years of age,[33–35] is associated with increased risk for long-term neurobehavioral disturbances. Additional well-designed studies are needed to develop a better understanding of anesthesia-induced developmental apoptosis, and to determine with reasonable certainty whether the human developing nervous system is susceptible to this type of injury.

Supplementary Material

Refer to Web version on PubMed Central for supplementary material.

Acknowledgments

Supported by National Institutes of Child Health and Human Development: HD37100, HD 052664, HD 062171 to JWO with subcontracts to AMB; National Institutes of Neurological Diseases and Stroke: 1RO1NS054044, R37NS045737-06S1/06S2 to SAB and 1F30NS066704 to AR; a Bugher Award and Grant in Aid from the American Heart Association (SAB), the March of Dimes Birth Defects Foundation (SAB), and RR-000163 for operation of the Oregon National Primate Research Center.

References

1. Ikonomidou C, Bosch F, Miksa M, et al. Blockade of NMDA receptors and apoptotic neurodegeneration in the developing brain. Science. 1999; 283:70–4. [PubMed: 9872743]
2. Ikonomidou C, Bittigau P, Ishimaru MJ, et al. Ethanol-induced apoptotic neurodegeneration and fetal alcohol syndrome. Science. 2000; 287:1056–60. [PubMed: 10669420]
3. Bittigau P, Sifringer M, Genz K, et al. Antiepileptic drugs and apoptotic neurodegeneration in the developing brain. Proc Natl Acad Sci USA. 2002; 99:15089–94. [PubMed: 12417760]
4. Jevtovic-Todorovic V, Hartman RE, Izumi Y, et al. Early exposure to common anesthetic agents causes widespread neurodegeneration in the developing rat brain and persistent learning deficits. J Neurosci. 2003; 23:876–82. [PubMed: 12574416]
5. Olney JW, Tenkova T, Dikranian K, et al. Ethanol-induced apoptotic neurodegeneration in the developing C57BL/6 mouse brain. Dev Brain Res. 2002; 133:115–26. [PubMed: 11882342]
6. Rizzi S, Carter LB, Ori C, Jevtovic-Todorovic V. Clinical anesthesia causes permanent damage to the fetal guinea pig brain. Brain Pathol. 2008; 18:198–210. [PubMed: 18241241]
7. Rizzi S, Ori C, Jevtovic-Todorovic V. Timing versus duration: determinants of anesthesia-induced developmental apoptosis in the young mammalian brain. Ann NY Acad Sci. 2010; 1199:43–51. [PubMed: 20633108]
8. Slikker W Jr, Zou X, Hotchkiss CE, et al. Ketamine-induced neuronal cell death in the perinatal rhesus monkey. Toxicol Sci. 2007; 98:145–58. [PubMed: 17426105]
9. Zou X, Patterson TA, Divine RL, et al. Prolonged exposure to ketamine increases neurodegeneration in the developing monkey brain. Int J Dev Neurosci. 2009; 27:727–31. [PubMed: 19580862]
10. Zou X, Liu F, Zhang X, et al. Inhalation anesthetic-induced neuronal damage in the developing rhesus monkey. Neurotoxicol Teratol. 2011; 33:592–597. [PubMed: 21708249]
11. Brambrink AM, Evers AS, Avidan MS, et al. Isoflurane-Induced Neuroapoptosis in the neonatal rhesus macaque brain. Anesthesiology. 2010; 112:834–841. [PubMed: 20234312]
12. Brambrink AM, Evers AS, Avidan MS, et al. Ketamine-induced neuroapoptosis in the fetal and neonatal rhesus macaque brain. Anethesiology. 2012; 116:372–84.
13. Farber NB, Creeley CE, Olney JW. Alcohol-induced neuroapoptosis in the fetal macaque brain. Neurobiol Dis. 2010; 40:200–206. [PubMed: 20580929]
14. Dobbing J, Sands J. Comparative aspects of the brain growth spurt. Early Hum Dev. 1979; 3:79–83. [PubMed: 118862]
15. Young C, Jevtovic-Todorovic V, Qin YQ. Potential of ketamine and midazolam, individually or in combination, to induce apoptotic neurodegeneration in the infant mouse brain. Brit J Pharmacol. 2005; 146:189–97. [PubMed: 15997239]
16. Cattano D, Young C, Straiko MMW, Olney JW. Subanesthetic doses of propofol induce neuroapoptosis in the infant mouse brain. Anesth Analg. 2008; 106:1712–4. [PubMed: 18499599]
17. Ma D, Williamson P, Januszewski A, et al. Xenon mitigates isoflurane-induced neuronal apoptosis in the developing rodent brain. Anesthesiology. 2007; 106:746–53. [PubMed: 17413912]
18. Johnson SA, Young C, Olney JW. Isoflurane-induced neuroapoptosis in the developing brain of non-hypoglycemic mice. J Neurosurg Anesth. 2008; 20:21–28.
19. Zhang X, Xue Z, Sun A. Subclinical concentration of sevoflurane potentiates neuronal apoptosis in the developing C57BL/6 mouse brain. Neurosci Lett. 2008; 447:109–14. [PubMed: 18852026]
20. Cattano, D.; Straiko, MMW.; Olney, JW. Chloral hydrate induces and lithium prevents neuroapoptosis in the infant mouse brain. Am Soc Anesthesiol Annual Meeting. 2008. Abstr. #A315 pub online at www.asaabstracts.com
21. Wozniak DF, Hartman RE, Boyle MP, et al. Apoptotic neurodegeneration induced by ethanol in neonatal mice is associated with profound learning/memory deficits in juveniles followed by progressive functional recovery in adults. Neurobiol Dis. 2004; 17:403–14. [PubMed: 15571976]
22. Satomoto M, Satoh Y, Terui K, et al. Neonatal exposure to sevoflurane induces abnormal social behaviors and deficits in fear conditioning in mice. Anesthesiol. 2009; 110:628–637.

23. Fredriksson A, Archer T, Alm H, et al. Neurofunctional deficits and potentiated apoptosis by neonatal NMDA antagonist administration. Behav Brain Res. 2004; 153:367–76. [PubMed: 15265631]
24. Fredriksson A, Archer T. Neurobehavioural deficits associated with apoptotic neurodegeneration and vulnerability for ADHD. Neurotox Res. 2004; 6:435–56. [PubMed: 15639778]
25. Fredriksson A, Ponten E, Gordh T, Eriksson P. Neonatal exposure to a combination of N-methyl-d-aspartate and γ-aminobutyric acid type A receptor anesthetic agents potentiates apoptotic neurodegeneration and persistent behavioral deficits. Anesthesiol. 2007; 107:427–36.
26. Stratmann G, May LD, Sall JW, et al. Effect of hypercarbia and isoflurane on brain cell death and neurocognitive dysfunction in 7 day-old rats. Anesthesiol. 2009; 110:849–61.
27. Stratmann G, Sall J, May LD, et al. Isoflurane differentially affects neurogenesis and long-term neurocognitive function in 60-day-old and 7-day-old rats. Anesthesiol. 2009; 110:834–48.
28. Sanders RD, Xu J, Shu Y, et al. Dexmedetomidine attenuates isoflurane-induced neurocognitive impairmert in neonatal rats. Anesthesiol. 2009; 110:1077–85.
29. DiMaggio C, Sun LS, Kakavouli A, Burne MW, Li G. A retrospective cohort study of the association of anesthesia and hernia repair surgery with behavioral and developmental disorders in young children. J Neurosurg Anesthesiol. 2009; 4:286–291. [PubMed: 19955889]
30. DiMaggio, C.; Sun, LS.; Li, G. Early childhood exposure to anesthesia and risk of developmental and behavioral disorders in a birth cohort of 5824 twin pairs. Abstr ISS-A1. Presented at International Safekids Symposium, International Anesthesiology Research Society Meeting; 2010. Available online at http://www.iars.org/abstracts/abstract_listings.asp
31. DiMaggio C, Sun L, Li G. Early childhood exposure to anesthesia and risk of developmental and behavioral disorders in a sibling birth cohort. Anesth Analg. 2011; 113:1143–51. [PubMed: 21415431]
32. Thomas, JJ.; Choi, JW.; Bayman, EO.; Kimble, KK.; Todd, MM.; Block, RI. Does anesthesia exposure in infancy affect academic performance in childhood? Abstract ISS-A4. Presented at International Safekids Symposium, International Anesthesiology Research Society Meeting; 2010. Available online at IARS.Org, Safekids, Science Symposium Program & Abstracts
33. Wilder RT, Flick RP, Sprung J, et al. Early Exposure to Anesthesia and Learning Disabilities in a Population-based Birth Cohort. Anesthesiology. 2009; 110:796–804. [PubMed: 19293700]
34. Flick RP, Katusic SK, Colligan RC, et al. Cognitive and behavioral outcomes after early exposure to anesthesia and surgery. Pediatrics. 2011; 128:e1053–61. [PubMed: 21969289]
35. Sprung J, Flick RP, Katusic SK, et al. Attention-deficit/hyperactivity disorder after early exposure to procedures requiring general anesthesia. Mayo Clin Proc. 2012; 87(2):120–129. [PubMed: 22305025]
36. Paule MG, Li M, Allen RR, et al. Ketamine anesthesia during the first week of life can cause long-lasting cognitive deficits in rhesus monkeys. Neurotoxicol Teratol. 2011; 33:220–30. [PubMed: 21241795]
37. Olney JW, Tenkova T, Dikranian K, et al. Ethanol-induced caspase-3 activation in the in vivo developing mouse brain. Neurobiol Dis. 2002; 9:205–19. [PubMed: 11895372]
38. Kitada M, Rowitch DH. Transcription factor co-expression patterns indicate heterogeneity of oligodendroglial subpopulations in the adult spinal cord. Glia. 2006; 54:35–46. [PubMed: 16673374]
39. Back SA, Luo NL, Borenstein NS, et al. Late oligodendrocyte progenitors coincide with the developmental window of vulnerability for human perinatal white matter injury. J Neurosci. 2001; 22:1302–1312. [PubMed: 11160401]
40. Riddle A, Luo N, Manese M, Beardsley D, Green L, Rorvik D, et al. Spatial heterogeneity in oligodendrocyte lineage maturation and not cerebral blood flow predicts fetal ovine periventricular white matter injury. J Neurosci. 2006; 26:3045–55. [PubMed: 16540583]
41. Rasband MN. The axon initial segment and the maintenance of neuronal polarity. Nat Rev Neurosci. 2010; 11:552–562. [PubMed: 20631711]
42. Back SA, Han BH, Luo NL, et al. Selective vulnerability of late oligodendrocyte progenitors to hypoxia-ischemia. J Neurosci. 2002; 22:455–63. [PubMed: 11784790]

43. Buser JR, Maire J, Riddle A, et al. Myelination failure in human perinatal white matter injury: Arrested pre-oligodendrocyye maturation contributes to myelination failure in premature infants. Ann Neurol. 2012; 71:93–109. [PubMed: 22275256]
44. Favrais G, van de Looij Y, Fleiss B, et al. Systemic inflammation disrupts the developmental program of the white matter. Ann Neurol. 2011; 70:550–565. [PubMed: 21796662]
45. Segovia KN, McClure MM, Moravec M, et al. Arrested oligodendrocyte lineage maturation in chronic perinatal white matter injury. Ann Neurol. 2008; 63:517–526.
46. Meador KJ. NEAD Study Group. Cognitive function at 3 years of age after fetal exposure to antiepileptic drugs. N Engl J Med. 2009; 360:1597–605. [PubMed: 19369666]
47. Banach R, Boskovic R, Einarson T, Koren G. Long-term developmental outcome of children of women with epilepsy, unexposed or exposed prenatally to antiepileptic drugs: a meta-analysis of cohort studies. Drug Saf. 2010; 33:73–9. [PubMed: 20000869]
48. Marlow N. Neurocognitive outcome after very preterm birth. Arch Dis Child Fetal Neonatal Ed. 2004; 89:224–8.
49. Jakovcevski I, Filipovic R, Mo Z, et al. Oligodendrocyte development and the onset of myelination in the human fetal brain. Front Neuroanat. 2009; 3:5. [PubMed: 19521542]
50. Shelton KL, Nicholson KL. GABA(A) positive modulator and NMDA antagonist-like discriminative stimulus effects of isoflurane vapor in mice. Psychopharmacol. 2010; 212:559–69.
51. Brosnan RJ. GABA(A) receptor antagonism increases NMDA receptor inhibition by isoflurane at a minimum alveolar concentration. Vet Anaesth Analg. 2011; 38:231–9. [PubMed: 21492389]
52. Riley EP, McGee CL. Fetal alcohol spectrum disorders: an overview with emphasis on changes in brain and behavior. Exp Biol Med. 2005; 230:357–65.
53. Olney JW, Young C, Qin Y-Q, et al. Ethanol-induced developmental glioapoptosis in mice and monkeys. Soc Neurosci Abst. 2005:Abst # 916.7.
54. Mattson SN, Riley EP, Sowell ER, et al. A decrease in the size of the basal ganglia in children with fetal alcohol syndrome. Alcohol Clin Exp Res. 1996; 20:1088–93. [PubMed: 8892532]
55. Ikonomidou C, Scheer I, Wilhelm T, et al. Brain morphology alterations in the basal ganglia and the hypothalamus following prenatal exposure to antiepileptic drugs. Eur J Paediatr Neurol. 2007; 11:297–301. [PubMed: 17418601]

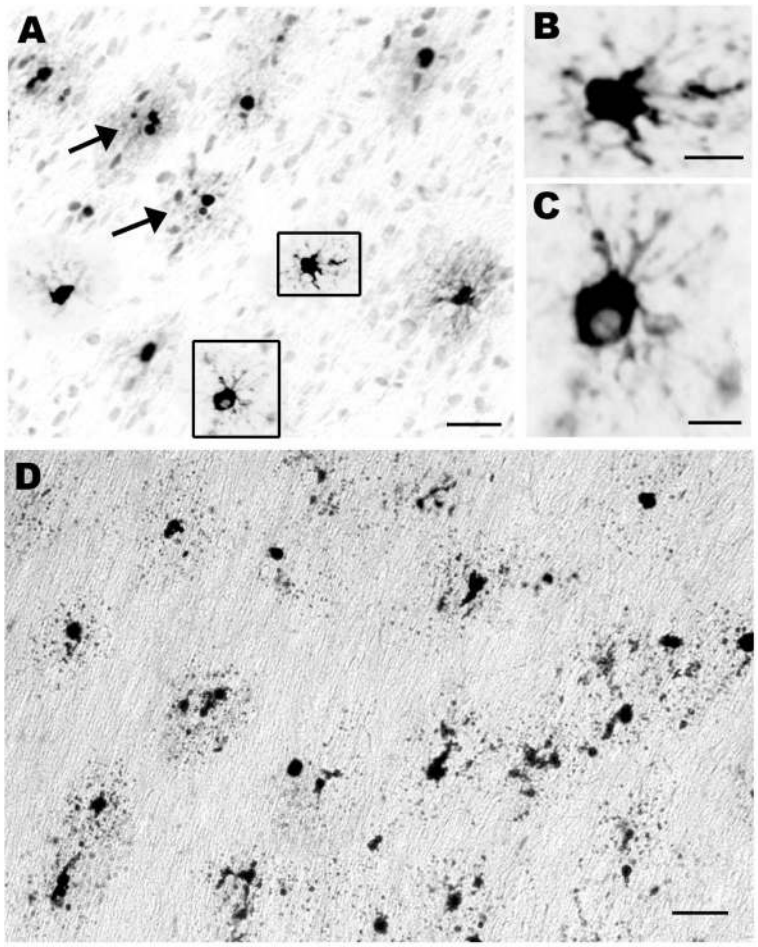

FIGURE 1.

Bright field images of the corpus callosum of an isoflurane-exposed brain stained with AC3 antibodies (A,B,C), or by the DeOlmos silver stain (D). Some of the profiles stained by AC3 (panel A) display multiple small condensed fragments (arrows), a sign of advanced apoptotic degeneration. Cells in an earlier stage (boxed) are shown at higher magnification in B & C. All of the cells stained by silver show signs of disintegration and are surrounded by a halo of particulate debris, signifying that the silver stain detects late, but not early, stages of degeneration. Scale bar = 25 μM for A; 10 μM for B and C.

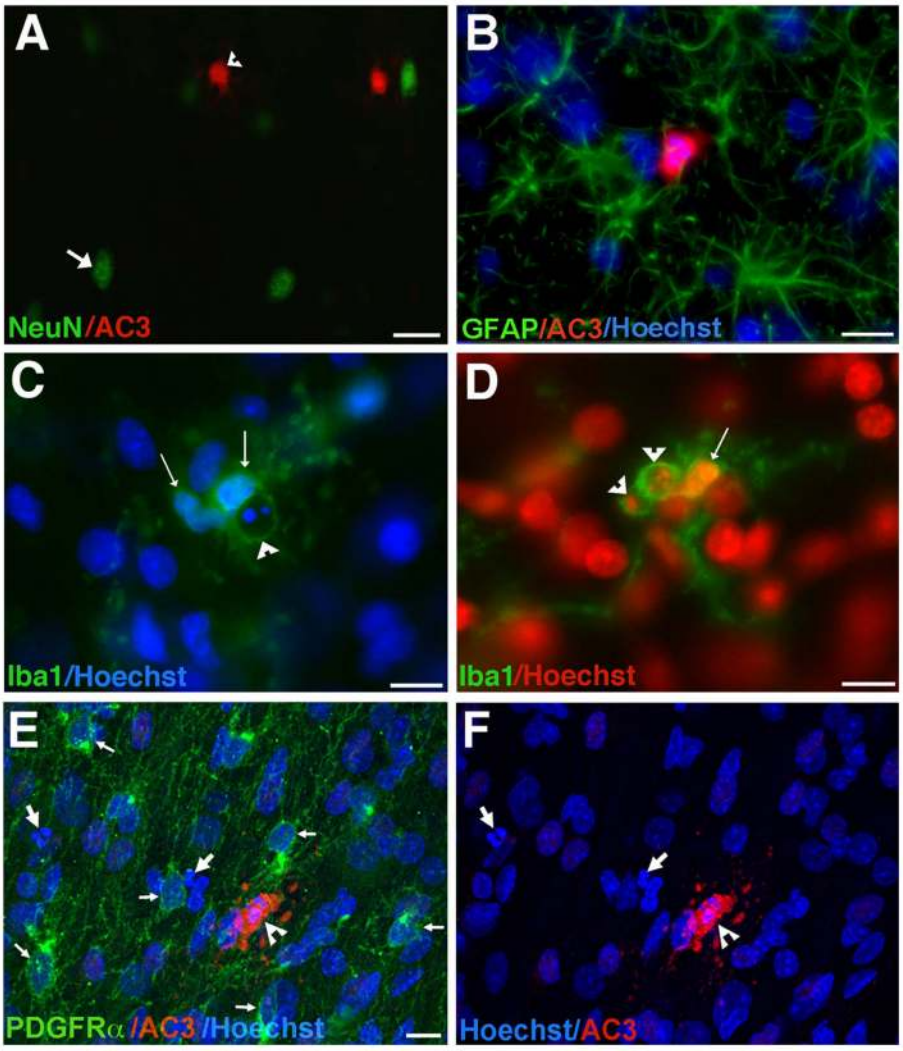

FIGURE 2.

Isoflurane-resistant cell types in neonatal monkey cerebral white matter. A. Interstitial white matter neurons, identified with NeuN (green nuclei; arrows) were a distinct population from AC3-labeled cells (red; arrowheads). B. GFAP-labeled astrocyte somata and processes had normal-appearing morphology (green) and did not co-localize with cells labeled with AC3 (red). C, D. Morphological features of Iba1-labeled activated phagocytic microglia (green). Most degenerating nuclei in the white matter were co-localized to microglia with reactive-appearing features. In C, a fragmented nucleus (Hoechst-labeled; blue; arrowhead) is contained within a bleb of membrane. Note the intact-appearing nuclei (arrows) of this and an adjacent cell. In D, multiple fragments of condensed chromatin (arrowheads; Hoechst, red pseudo-color for improved contrast) were distributed within two blebs of membrane of this cell with an intact nucleus (arrow). Note the thickened processes of this activated-appearing cell. E, F. Numerous PDGFRα-labeled OL progenitors (green; thin arrows) were visualized throughout the corona radiata and did not stain for AC3 (red; arrowhead). Note that the nuclei of the OL progenitors appeared intact in contrast to adjacent nuclei visualized with Hoechst (blue, thick arrows in E, F) that displayed features of apoptotic degeneration with condensed and fragmented chromatin. Bars= 50 μm (A); 25 μm (B, C); 10 μm (D, E, F).

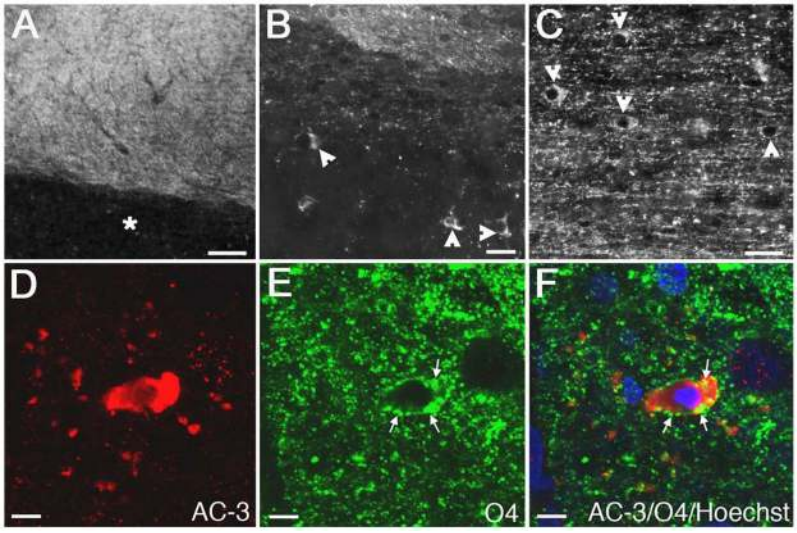

FIGURE 3.

Immature oligodendrocytes in myelinating neonatal white matter tracts degenerate in response to isoflurane exposure. (A) Neonatal cerebral white matter tracts were heavily myelinated, as visualized with the O4 antibody and the O1 antibody (not shown). Myelination was not observed in the deep cerebral cortical gray matter (asterisk). (B) At the edge of myelinating white matter tracts, scattered immature OLs were visualized with both the O4 antibody (arrowheads) and the O1 antibody (not shown). (C) Within heavily myelinated tracts, O4-labeled cells were visualized (arrowheads). Hoechst 33342 visualized the nucleus within the cell bodies (not shown). (D-F) Confocal microscopy confirmed that O4-labeled immature OLs were AC3-positive. (D) Degenerating AC3-labeled cell with a halo of degenerating processes. (E) Distribution of O4 staining shows the abundant myelination corresponding to the region shown in D. Note the increased O4 staining around the plasma membrane of a cell (arrows). (F) Merge of D and E. Bars = 100 μm (A); 25 μm (B, C); 10 μm (D–F).

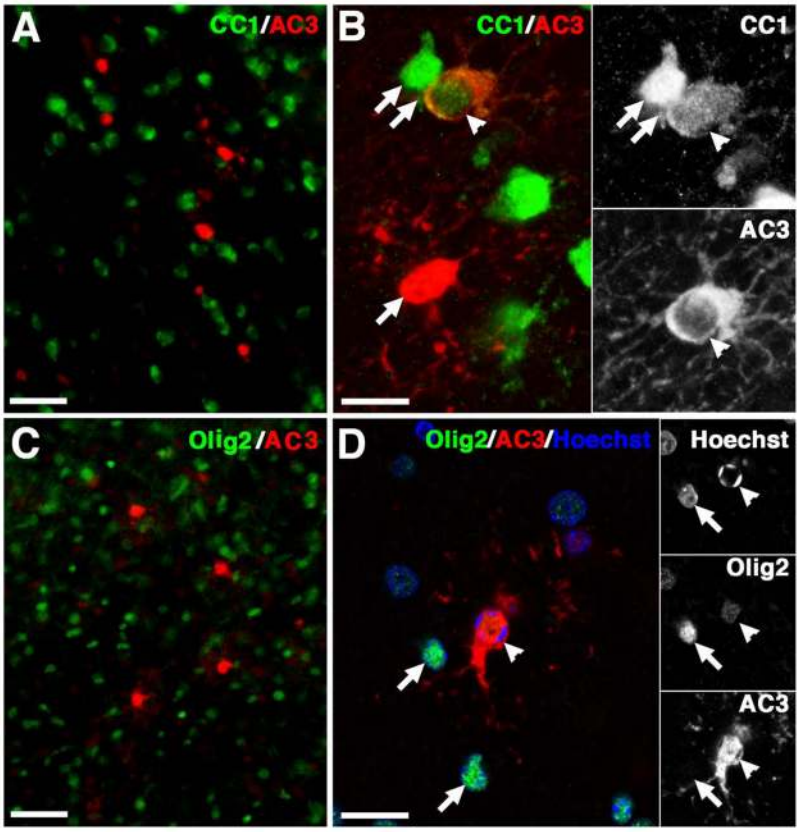

FIGURE 4.

Mature oligodendrocytes in myelinating neonatal white matter tracts degenerate in response to isoflurane exposure. (A, C) As visualized by epi-fluorescence microscopy, AC3-labeled cells at various stages of degeneration (red) did not appear to co-localize with cells labeled with the OL-lineage specific markers, CC-1 (A) and Olig 2 (C). (B) By confocal microscopy, the mature OL marker CC-1 (green) was robustly visualized in the cytoplasm of intact appearing cells (double arrow). Two AC3-positive cells were visualized at different stages of degeneration. One cell at an earlier stage (arrowhead) had intact appearing processes (see AC3 black/white inset) and was less intensely stained for AC3 and stained more weakly for CC-1 than adjacent intact cells (double arrow). Another cell at a more advanced stage of degeneration (arrow) displayed degenerating processes, more robust AC3 staining than the cell at an earlier stage of degeneration (double arrows) and had no apparent CC-1 staining. (D) As shown by confocal microscopy, some intact appearing nuclei (blue) strongly co-localized with Olig2 (green) (arrows) and did not label for AC3 (red). By contrast (black and white insets), a degenerating OL (arrowhead) had a pyknotic nucleus with fragmented chromatin (Hoechst), more weakly labeled with Olig 2 and double-labeled with AC3. Bars = 100 μM (A, C); 15 μM (B) and 25 μM (D).

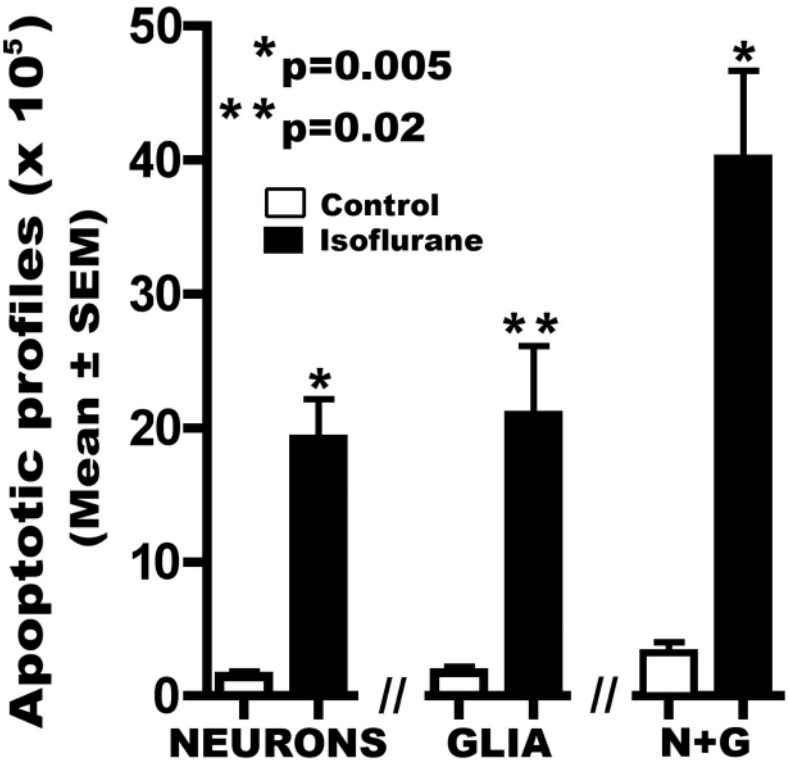

FIGURE 5.

Total numbers of apoptotic neurons or glia, or neurons + glia (N+G) per brain (mean ± SEM) of P6 rhesus neonates exposed to isoflurane or to no drug (control). All of the values for the isoflurane-exposed brains were significantly higher than those for the control brains at the significance levels indicated. The mean number of apoptotic neurons (19.14 × 105) was slightly less that the mean number of apoptotic glia (20.89 × 10^5), yielding a neuron to glia ratio of 48 to 52.

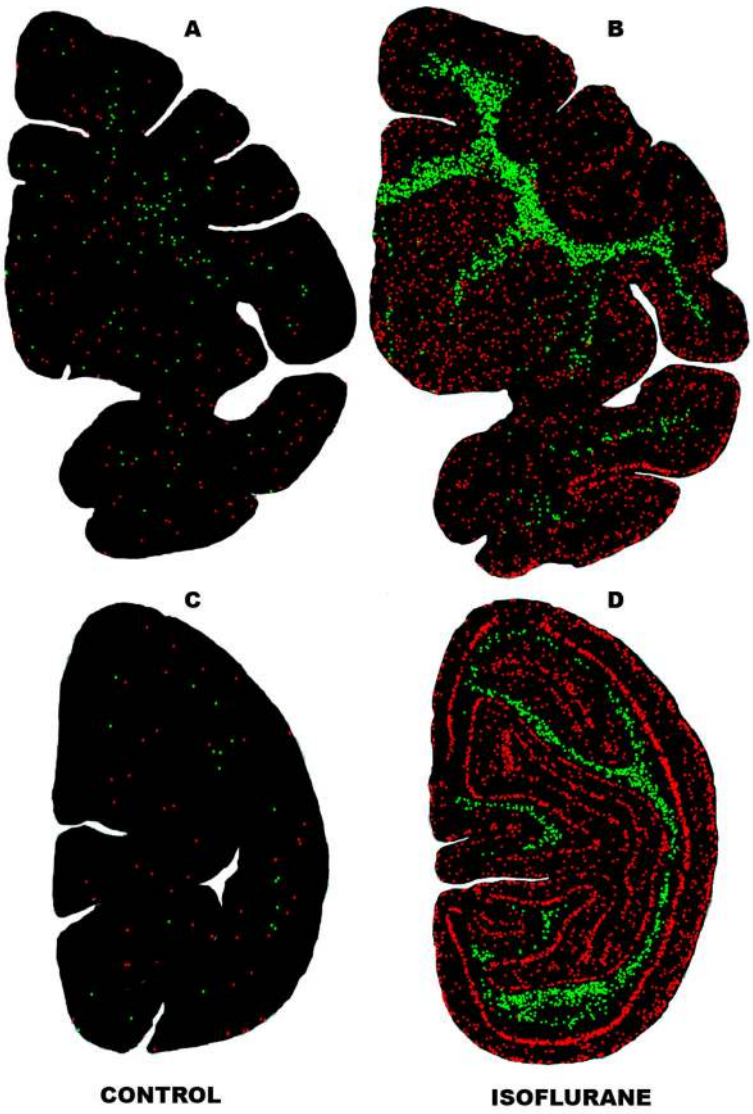

FIGURE 6.

Computer plots showing the distribution of apoptotic neurons (red dots) and apoptotic glia (green dots) in sections cut at a mid rostro-caudal level (A and B), or at the level of the primary visual (occipital) cortex (C and D). The control brain has sparse numbers of apoptotic profiles and there is no pattern of concentration in any particular region, except that the glial profiles are more concentrated in white matter and the neuronal profiles are enriched in gray matter. In contrast, the apoptotic profiles in the isoflurane-exposed brain are much more abundant, with glia being heavily concentrated in white matter zones, and neurons showing dense packing in specific gray matter areas. Note the highly organized laminar pattern in some regions, especially the visual cortex, reflecting the known location of layer II and layer V neurons.

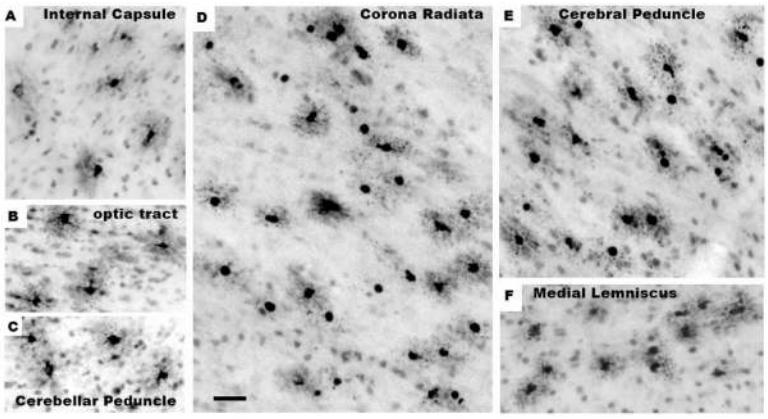

Figure 7.

Isoflurane induced diffuse glial degeneration throughout the neuraxis as demonstrated by brightfield images of apoptotic glia stained with antibodies to AC3. All images were acquired at the same magnification and demonstrate the relative density of degenerating cells in the representative white matter tracts shown. The staining in the frontal corona radiata is representative of that in the prefrontal, parietal, temporal and occipital cortices. The cerebral peduncle is shown at the level of the midbrain basilar division. The cerebellar peduncle staining is from the middle division situated between the peduncle and the deep cerebellar nuclei. The optic tract is in the diencephalon and the medial lemniscus is in the medula oblongata. Scale bar in D = 25 μM for all panels.